

Original Article

***Tripterygium hypoglaucum* (Levl.) Hutch attenuates oleic acid-induced acute lung injury in rats through up-regulating claudin-5 and ZO-1 expression**

Ping Shao^{1,3*}, Jinyuan Zhu^{2*}, Huan Ding², Wenjie Zhou², Wenyan Zhou², Qinfu Liu², Yuangui Li², Xigang Ma²

¹Department of Respiratory Medicine, The Second Affiliated Hospital of Ningxia Medical University, Yinchuan, Ningxia Hui Autonomous Region, China; ²Department of Critical Care Medicine, General Hospital of Ningxia Medical University, Yinchuan City 750004, Ningxia Hui Autonomous Region, China; ³Yinchuan First People's Hospital, Yinchuan City 750001, Ningxia Hui Autonomous Region, China. *Equal contributors.

Received September 13, 2017; Accepted January 16, 2018; Epub July 15, 2018; Published July 30, 2018

Abstract: *Tripterygium hypoglaucum* (Levl.) Hutch (THH), a perennial plant, has shown multiple pharmacological actions; however, there is little knowledge on the activity against lung injury. This study aimed to evaluate the effect of THH on oleic acid-induced acute lung injury (ALI) in rats and explore the underlying mechanisms. Male SD rats were randomly assigned to 5 groups. Rats in the ALI group ($n = 15$) were orally administered 2 ml of 0.9% physiological saline for 10 successive days, and then ALI was induced in the rats by injection of 0.04 ml/kg oleic acid into the tail vein 1 h after the last oral administration. Animals in the low-, moderate-, and high-dose THH groups were orally administered THH tablets at daily doses of 500, 600, and 700 mg/kg for successive 10 days, and then oleic acid was given at a dose of 0.04 ml/kg by tail vein injection 1 h after the last oral administration. The control rats were given 2 ml 0.9% physiological saline by gavage for 10 successive days, and physiological saline was given at a dose of 0.04 ml/kg by tail vein injection 1 h after the last oral administration. Claudin-5 and ZO-1 expression was determined in rat lung tissues using immunohistochemistry, qRT-PCR, and Western blotting assays, and the lung wet/dry (W/D) weight ratio and lung permeability index (LPI) were measured. Rat lung tissue morphology was observed using HE staining and a lung injury score was estimated, while the ultra-structural changes of the rat lung tissues were visualized using transmission electronic microscopy (TEM). Significantly lower claudin-5 and ZO-1 expression was detected in the ALI group than in the control group at both translational and transcriptional levels ($P < 0.05$), and the claudin-5 and ZO-1 protein expression was higher in the three THH groups than in the ALI group ($P < 0.05$). A significant rise was seen in the lung W/D weight ratio, LPI, and LIS in the ALI group in relative to the control group, while THH treatment resulted in a significant reduction in lung W/D weight ratio, LPI, and LIS as compared to the ALI group in a dose-dependent manner. However, no significant differences were found between the low- and moderate-dose THH groups ($P > 0.05$). Microscopy showed obvious rat lung injury in the ALI group, with edema and intracellular junction disorganization seen in lung tissues. The results of the present study demonstrate that THH attenuates pulmonary vascular endothelial cell injury caused by ALI through up-regulation of claudin-5 and ZO-1 expression, and dose-dependent protection of the lung barrier function. Our findings indicate that claudin-5 and ZO-1 may be potential targets for treatment of ALI.

Keywords: *Tripterygium hypoglaucum*, root extract, acute lung injury, tight junction protein, lung barrier function

Introduction

Acute lung injury (ALI) is a lung disorder caused by multiple direct and indirect factors, such as wound, shock, severe infections, sepsis, and hypoxia [1-3]. Acute respiratory distress syndrome (ARDS), a severe form of ALI, is characterized by diffuse lung inflammation and severe hypoxemia [4]. A variety of therapies have been developed for ARDS so far [5]; however, only low-tidal-volume ventilation is effective to

reduce mortality due to ARDS [6-8]. In addition, glucocorticoids are active against inflammation but have a high toxicity, which is ineffective for improving the prognosis and mortality of ARDS [9-11]. Development of novel therapeutic targets, is therefore of great need for the treatment of ALI.

Previous studies have demonstrated the anti-inflammatory, immunosuppressive, anti-fertility, anti-viral, and anti-tumor roles of the tradi-

T. hypoglaucum attenuates acute lung injury

tional Chinese herbal medicine *Tripterygium hypoglaucum* (Levl.) Hutch (THH) [12-17], and the agent has been used for clinical treatment of nephrotic syndrome, rheumatoid arthritis, and erosive oral lichen planus [18-20]. In addition, THH has been found to alleviate inflammatory exudation and regulate immune response [21]. However, there is little known about the effect of THH on ALI. The present study was therefore designed using a rat model, to evaluate the effect of THH on oleic acid-induced ALI and explore the underlying mechanisms.

Materials and methods

Animals and grouping

Seventy male 6 to 7 weeks-old healthy rats of the SD strain, each weighing 200 ± 20 g, were purchased from the Laboratory Animal Center of Ningxia Medical University (Yinchuan, China). Rats were maintained at $22 \pm 2^\circ\text{C}$ in a relative humidity of 60% under a 12-h light/12-h dark cycle, of 3 to 4 animals in each cage. All rats were randomly assigned to 5 groups. Rats in the ALI group ($n = 15$) were orally administered with 2 ml 0.9% physiological saline (China Otsuka Pharmaceutical Co., Ltd.; Tianjin, China) twice daily for successive 10 days, and then ALI was induced in rats by injection of 0.04 ml/kg oleic acid (99.9% purity, Tianjin Guangfu Fine Chemical Institute; Tianjin, China) into the tail vein 1 h after the last oral administration [22]. Animals in the low-, moderate- and high-dose THH groups were given THH solution [THH tablets (Chongqing Academy of Chinese Materia Medica; Chongqing, China) were pieced and dissolved in 2 ml 0.9% physiological saline] by gavage at daily doses of 500, 600, and 700 mg/kg for successive 10 days, and then oleic acid was given at a dose of 0.04 ml/kg by tail vein injection 1 h after the last oral administration. The control rats were administered with 2 ml 0.9% physiological saline twice daily for successive 10 days, and physiological saline was given at a dose of 0.04 ml/kg by the tail vein injection 1 h after the last oral administration.

Measurement of lung wet/dry (W/D) weight ratio and lung permeability index (LPI)

Rats were anaesthetized by intraperitoneal injection of 10% chloral hydrate (purity, 99.5%; Tianjin Damao Chemical Reagent Factory, Tianjin, China) at a dose of 0.3 ml/100 mg 4 h

after animal modeling. Blood was sampled from the rat abdominal aorta and bronchoalveolar lavage fluid (BALF) was prepared. Briefly, the rat chest wall was incised, and the bilateral lungs were exposed. The right pulmonary hilum was then ligated, and the neck was incised to expose the trachea. A 5Fr plastic endotracheal catheter (approximately 2 mm in diameter and 1.2 mm in inner diameter; Shenzhen Corigo Medical Instrument Co., Ltd.; Shenzhen, China) was inserted into the trachea, and fixed with threads. The catheter was injected with physiological saline for bronchoalveolar lavage, and 8 to 10 ml of BALF was recovered. The BALF was then filtered through double-layer gauze, centrifuged at 4°C , 4000 r/min for 10 min, and the supernatant was collected. The protein concentration in plasma and BALF was quantified using a BCA protein assay kit (Nanjing KeyGen Biotech Co., Ltd.; Nanjing, China). LPI was calculated using the following formula: $\text{LPI} = \frac{\text{protein concentration in BALF}}{\text{protein concentration in plasma}}$. The middle lobe of the right lung was collected, and rinsed with physiological saline. Following removal of water and blood from the surface with filter paper, the middle lobe was weighed and dried at 80°C in a 202-2 electrothermal constant-temperature drying box (Shanghai Experimental Instrument Co., Ltd.; Shanghai, China) for 72 h to constant weight, and the lung W/D weight ratio was estimated.

Histological examinations

After 4 h of animal modeling, the rats were anaesthetized by intraperitoneal injection of 10% chloral hydrate at a dose of 0.3 ml/100 mg, and sacrificed. The lower lobe of the right lung was collected (weighing 0.24 to 0.53 g), fixed in 4% paraformaldehyde, embedded in paraffin wax, cut into sections, stained with hematoxylin-eosin (HE), and visualized under an Olympus BX51 optical microscope (Olympus Co.; Tokyo, Japan) at a magnification of $\times 400$. Lung injury was assessed in a blind manner, grading the histological findings of alveolar edema, interstitial edema, peripheral edema, alveolar edema combined with peripheral edema, and alveolar edema combined with presence of interstitial inflammatory cells on lung tissue sections, each on a scale of 1-4: 1, normal; 2, mildly severe injury; 3, moderately severe injury; and 4, highly severe injury [23]. The lung injury score (LIS) was calculated for

Table 1. Primers used for the qRT-PCR assay

Gene	Primer sequence
Claudin-5	Forward 5'-TTGGAAGGGGCTGTGGAT-3'
	Reverse 5'-GGAAACTGAACCTCGACGC-3'
ZO-1	Forward 5'-TGCTATTACAGGTCCTC-3'
	Reverse 5'-TGGTGCTCCTAAACAATC-3'
β -actin	Forward 5'-GAGAGGGAAATCGTGCGTGAC-3'
	Reverse 5'-CATCTGCTGGAAGGTGGACA-3'

each section by averaging 10 randomly selected fields under $\times 400$.

Immunohistochemistry

After 4 h of animal modeling, the rats were anaesthetized by intraperitoneal injection of 10% chloral hydrate at a dose of 0.3 ml/100 mg, and sacrificed. The lower lobe of the right lung was collected (weighing 0.15 to 0.24 g), fixed in 4% paraformaldehyde, embedded in paraffin wax and cut into sections. Paraffin wax-embedded lung tissue sections were routinely dewaxed, rehydrated, antigen-retrieved, blocked in goat serum, incubated in rabbit anti-mouse claudin-5 monoclonal antibody (1:200; Abcam; Cambridge, MA, USA) and rabbit anti-mouse ZO-1 polyclonal antibody (1:400; Abcam; Cambridge, MA, USA) at 4°C overnight, while negative controls were incubated in PBS. Sections were then rinsed with PBS, incubated in goat anti-rabbit horseradish peroxidase (HRP)-conjugated IgG secondary antibody (1:1000; Abcam; Cambridge, MA, USA) for 60 min in a wet box, rinsed with PBS, stained with DAB, re-stained with HE for 3 min, dehydrated with a graded series of alcohol, made transparent with xylene, and mounted with neutral resins. Sections were then visualized using microscopy at a magnification of $\times 400$, and images were captured using the image capturing system DP Controller version 3.1.1.267. Three sections were selected for each rat in each group, and five fields of vision were randomly selected on each section.

qRT-PCR assay

After 4 h of animal modeling, the rats were anaesthetized by intraperitoneal injection of 10% chloral hydrate at a dose of 0.3 ml/100 mg, and sacrificed. The lower lobe of the right lung was collected (weighing 0.19 to 0.28 g).

100 mg of right lung tissues were ground in a liquid nitrogen precooled grinder. Total RNA was then extracted using a Trizol RNA extraction kit (Invitrogen; Carlsbad, CA, USA) and transcribed into cDNA with a Reverse Transcription Kit (Beijing TransGen Biotech Co., Ltd.; Beijing, China). Claudin-5 and ZO-1 mRNA expression was determined using a qRT-PCR assay in a 20 μ L system containing 0.5 μ L of cDNA template, 10 μ L of 2 \times SYBR Green qPCR Mix, 0.8 μ L of primers (10 μ mol/L) and 8.7 μ L of nuclease-free water under the following conditions: at 95°C for 10 min, and 42 cycles of at 95°C for 15 s and at 60°C for 1 min, while β -actin served as an internal control. All primers used for the qRT-PCR assay are described in **Table 1**. The relative mRNA quantity was calculated using the $2^{-\Delta\Delta Ct}$ method.

Western blotting assay

After 4 h of animal modeling, the rats were anaesthetized by intraperitoneal injection of 10% chloral hydrate at a dose of 0.3 ml/100 mg, and sacrificed. The lower lobe of the right lung was collected (weighing 0.11 to 0.25 g). Right lung tissues that were frozen at -80°C were lysed in cell lysis solution, homogenized on a glass homogenizer and centrifuged for protein extraction. The protein concentration was quantified using a BCA protein assay kit (Nanjing KeyGen Biotech Co., Ltd.; Nanjing, China). Total protein was separated using SDS-PAGE a 12% separating gel and a 5% stacking gel, and then the blots were electrotransferred to PVDF membrane (Millipore; Bedford, MA, USA) at 300 mA for 90 min. Following blocking in 5% fat-free milk powder for 60 min, the membrane was washed in TBST, incubated in rabbit anti-mouse claudin-5 monoclonal antibody (1:200), rabbit anti-mouse ZO-1 polyclonal antibody (1:300), or at 4°C overnight, while rabbit anti-GAPDH antibody (1:500; Cell Signaling Technology, Inc.; Beverly, MA, USA) served as a loading control. The membrane was then washed three times in TBST, 10 min each time, and incubated in goat anti-rabbit HRP-conjugated secondary antibody (1:5000; Beijing Zhongshan Golden Bridge Biotechnology Co., Ltd.; Beijing, China) at room temperature for 60 min. Following washing three times in TBST, 10 min each time, the immunoreactive bands were visualized using ECL, and analyzed with a JS-680D gel imaging analysis system (Shanghai

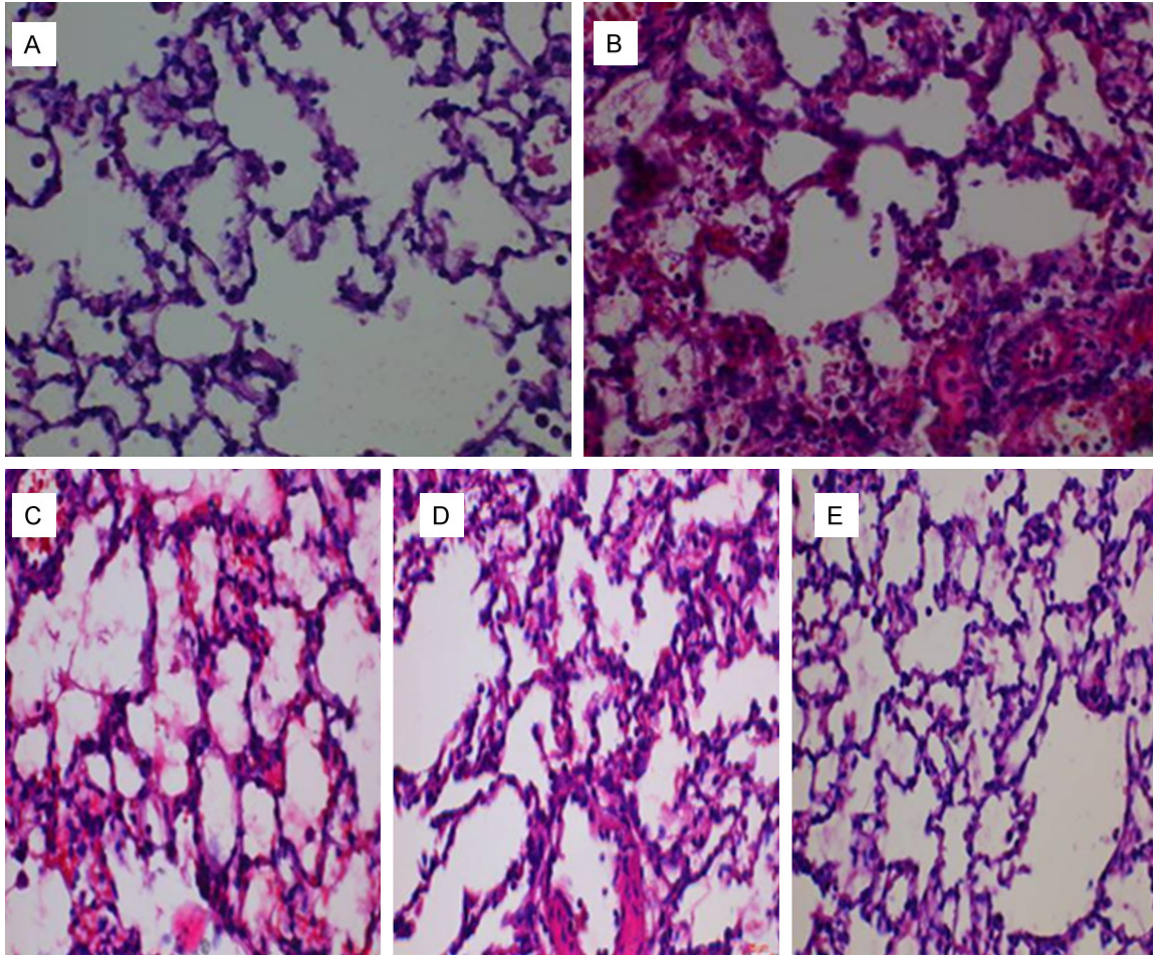


Figure 1. Pathological changes of rat lung tissues (HE staining, $\times 400$). (A) Normal control rats have intact and clear pulmonary alveolar structure without destruction, clean pulmonary alveolar cavity, no broadening, congestion, or edema of the pulmonary alveolar septum, no inflammatory cell infiltration, or bleeding; (B) the rats in the ALI group have remarkable broadening of the pulmonary alveolar wall, diffuse edema of pulmonary alveolus and interstitium, interstitial telangiectasia, alveolar collapse, significant inflammatory cell infiltration, and erythrocyte exudation in the pulmonary alveolar cavity and pulmonary interstitium, with a rise in the plasma protein exudation. The rats in the low- (C) and moderate-dose THH groups (D) have unclear pulmonary alveolar structure, pulmonary congestion and edema, and inflammatory cell and red blood cell infiltration in a part of the pulmonary alveolus and interstitium. The rats in the high-dose THH group (E) have almost clear alveolar structure, remarkable alleviation of pulmonary congestion and edema, and inflammatory cell and red blood cell infiltration is seen in a small portion of the pulmonary alveolus and interstitium.

Peiqing Science & Technology Co., Ltd.; Shanghai, China). Protein levels were normalized to GAPDH levels.

Ethical statement

This study was approved by the Ethical Review Committee of General Hospital of Ningxia Medical University (permission number: NZY-2013-0012). All animal experimentation was performed according to the Guidelines for Laboratory Animal Care and Management in China (2011[588]).

Statistical analysis

All measurement data are expressed as the mean \pm standard deviation (SD). Differences of normally distributed data among groups were tested for statistical significance with one-way analysis of variance (ANOVA), followed by the SNK-q test, while comparisons of non-normally distributed data were done using a non-parametric test following rank transformation. All statistical analyses were performed using the statistical software SPSS version 16.0 (SPSS, Inc.; Chicago, IL, USA), and a *P*

value < 0.05 was considered statistically significant.

Results

Effect of THH on lung morphology and ultra-structure in rats with oleic acid-induced ALI

The lung tissues appeared bright red in the control rats, with no apparent abnormal changes seen. Dark red lung tissues with poor elasticity were observed in the ALI group, with lung enlargement seen, and a great amount of pale red fluid exudates came out from the section, with pink liquid seen in the bronchus. The lung tissues showed mild swelling in three THH groups, with scattered bleeding spots seen on the lung surface, and a small amount of pale red fluid exudate came out from the section. In addition, there was no significant dose-specific variation seen in the lung appearance.

Optical microscopy showed intact and clear pulmonary alveolar structure without destruction, clean pulmonary alveolar cavity, no broadening, congestion or edema of the pulmonary alveolar septum, no inflammatory cell infiltration, or bleeding in the control rats. In the ALI group, the rats had remarkable broadening of the pulmonary alveolar wall, diffuse edema of pulmonary alveolus and interstitium, interstitial telangiectasia, alveolar collapse, a great deal of inflammatory cell infiltration and erythrocyte exudation in the pulmonary alveolar cavity and pulmonary interstitium, with a rise in the plasma protein exudation. The rats in the three THH groups had unclear pulmonary alveolar structure, pulmonary congestion, alleviation of edema, and mild inflammatory cell infiltration in a part of pulmonary alveolus and interstitium. Pathological lung injury was alleviated in the three THH groups relative to the ALI group, and there was no significant difference in lung injury between the low- and moderate-dose THH groups, with the greatest alleviation of pathological injury seen in the high-dose THH group (Figure 1).

Transmission electronic microscopy (TEM) showed normal pulmonary alveolar structure, normal morphology, and structure of microvascular endothelial cells and basement membrane, regular structure of alveolar type II epithelial cells, and irregular microvilli on alveolar surface, obvious nucleus, even cytoplasm, and

typical lamellar body (unequal number, irregular size and various degrees of maturity) in the cytoplasm in the control rats. We observed relatively irregular morphology of alveolar type II epithelial cells, alveolar type II epithelial cell degeneration and disruption, a reduction in the number and even disappearance of the microvilli on alveolar surface, and a remarkable increase in the lamellar body evacuation in the cytoplasm, which led to vacuolization in the ALI group. Also, exfoliative lamellar bodies, karyopycnosis, aggregation of alveolar type II epithelial cell chromatin into masses, obvious organelle destruction in pulmonary alveolus, mitochondrial cristae dissolution and disruption and even disappearance were also observed which resulted in vacuolization. In addition, we observed rough endoplasmic reticulum expansion, ribosome degranulation, increased amounts of lysosomes, and elevated amounts of collagen in pulmonary alveolar interstitium, with a large number of apoptotic cells. There was also severe swelling of the vascular endothelial cells, defective, disruptive, loose, and unclear basement membranes, chromatin aggregation, capillary occlusion, endothelial cell damage, exfoliation, and apoptosis. A large number of inflammatory cells was also found in the capillary vessel of the ALI group. The rats in the three THH groups had almost normal morphology of alveolar type II epithelial cells, recovery of microvilli on the alveolar surface, an increase in the number of lamellar bodies in the cytoplasm, a reduction in the vacuolization in the lamellar body, but normal organelles in the alveolar cells, despite slight swelling of microvascular endothelial cells with almost normal morphology, and intact basement membrane and unclear collagen hyperplasia. Moreover, TEM revealed a greater alleviation of ALI in the high-dose THH group than in the low- and moderate-dose THH groups (Figure 2).

A higher LIS was calculated in the ALI group than in the control group ($P < 0.01$), and lower LIS was observed in the three THH groups as compared to the ALI group ($P < 0.01$), however, the LIS was higher in the three THH groups relative to the control group ($P < 0.01$). In addition, a higher LIS was seen in the high-dose THH group than in the low- and moderate-dose THH groups ($P < 0.05$), while no significant difference was found in the LIS between the low- and moderate-dose THH groups ($P > 0.05$) (Table 2).

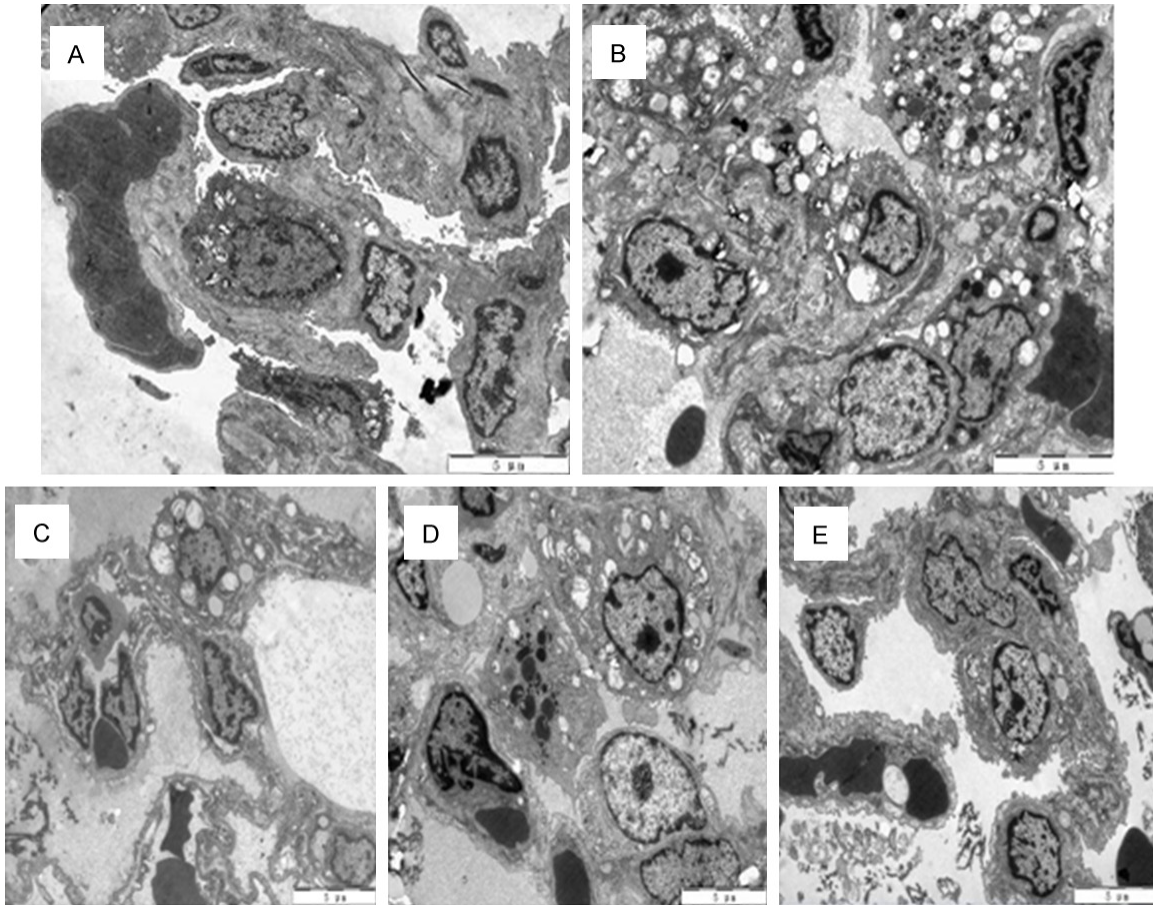


Figure 2. Ultrastructural changes of rat lung tissues (HE staining, $\times 400$). (A) Normal control rats have normal pulmonary alveolar structure, normal morphology, and structure of microvascular endothelial cells and basement membrane, regular structure of alveolar type II epithelial cells, and irregular microvilli on alveolar surface, obvious nucleus, even cytoplasm, and typical lamellar body (unequal number, irregular size and various degrees of maturity) in the cytoplasm. (B) Rats with oleic acid-induced ALI have relatively irregular morphology of alveolar type II epithelial cells, alveolar type II epithelial cell degeneration and disruption, a reduction in the number and even disappearance of the microvilli on alveolar surface, a remarkable increase in the lamellar body evacuation in the cytoplasm, which leads to vacuolization, and exfoliative lamellar body, karyopycnosis, aggregation of alveolar type II epithelial cell chromatin into masses, obvious organelle destruction in pulmonary alveolus, mitochondrial cristae dissolution, and disruption and even disappearance, resulting in vacuolization development. In addition, the ALI rats have rough endoplasmic reticulum expansion, ribosome degranulation, increased amounts of lysosome, elevated amounts of collagen in pulmonary alveolar interstitium, with a large number of apoptotic cells seen, severe swelling of vascular endothelial cells, defective, disruptive, loose and unclear basement membranes, chromatin aggregation, capillary occlusion, endothelial cell damage, exfoliation and apoptosis, and a large number of inflammatory cells in the capillary vessel. (C and D) Rats in the low- (C) and moderate-dose THH groups (D) have recovery of alveolar epithelial cell morphology, microvilli on alveolar surface, recovery of lamellar body in the cytoplasm, a reduction of the vacuolization in the lamellar body relative to the ALI group, normal organelle in alveolar cells, slight swelling of microvascular endothelial cells with almost normal morphology and intact basement membrane. (E) the rats in the high-dose THH group have almost normal morphology of alveolar type II epithelial cells, remarkable recovery of microvilli on alveolar surface, an increase in the number of lamellar body in the cytoplasm, a reduction in the vacuolization in the lamellar body, normal organelle in alveolar cells, slight swelling of microvascular endothelial cells with almost normal morphology, intact basement membrane, and unclear collagen hyperplasia.

Effect of THH on lung W/D weight ratio and LPI in rats with oleic acid-induced ALI

Significantly higher lung W/D weight ratio and LPI were measured in the ALI group than in the control group ($P < 0.01$), while significantly

lower lung W/D weight ratio and LPI were found in the three THH groups relative to the ALI group ($P < 0.01$). Higher lung W/D weight ratio and LPI were observed in low- and moderate-dose THH groups as compared to the control group ($P < 0.01$), while no significant differences were

T. hypoglaucum attenuates acute lung injury

Table 2. Lung wet/dry weight (W/D) ratio, lung permeation index (LPI) and lung injury score (LIS) in rats of various groups

Group	No. of animals	Lung wet/dry weight (W/D) ratio	Lung permeation index (LPI)	Lung injury score (LIS)
Control	10	4.44 ± 0.39	0.38 ± 0.052	0.40 ± 0.083
ALI	15	7.68 ± 0.64 [#]	0.89 ± 0.153 [#]	3.81 ± 0.424 [#]
H1	15	5.42 ± 0.44 ^{#,Δ}	0.60 ± 0.083 ^{#,Δ}	2.62 ± 0.483 ^{#,Δ}
H2	15	5.66 ± 0.63 ^{#,Δ,☆}	0.61 ± 0.056 ^{#,Δ,☆}	2.67 ± 0.337 ^{#,Δ,☆}
H3	15	4.62 ± 0.84 ^{Δ,▲}	0.46 ± 0.069 ^{Δ,▲}	1.22 ± 0.393 ^{#,Δ,▲}

[#]*P* < 0.01 vs. the control group; ^Δ*P* < 0.01 vs. the ALI group; [▲]*P* < 0.05 vs. the H1 group; [☆]*P* < 0.05 vs. the H2 group.

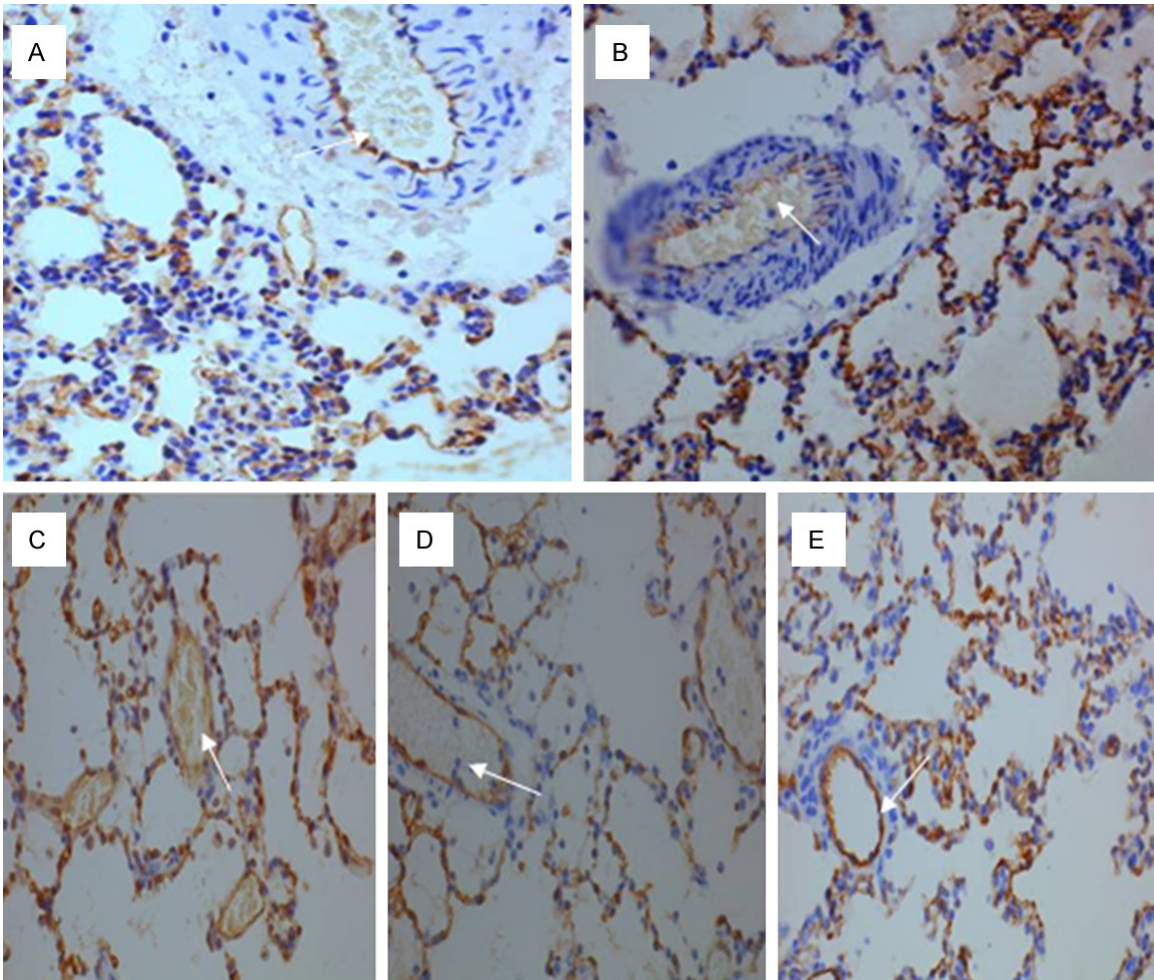


Figure 3. Immunohistochemical staining determines claudin-5 expression in rat lung tissues (× 400). (A) immunohistochemistry demonstrates moderately and highly positive claudin-5 expression (yellow brown) in pulmonary vascular endothelial cells and weakly positive expression in alveolar endothelial cells in the control group; (B) immunohistochemistry shows negatively or weakly positive claudin-5 expression in pulmonary vascular endothelial cells in the ALI group; (C-E) claudin-5 expression was increased with the rise in THH dose in the pulmonary vascular endothelial cells, and the highest claudin-5 expression was in the high-dose THH group (E) in relative to the low- (C) and moderate-dose THH groups (D). In addition, weakly positive claudin-5 expression was detected in the alveolar endothelial cells in the low-dose THH group, and the level of claudin-5 expression was comparable between the high-dose THH group and the control group.

detected between the high-dose THH group and the control group (*P* > 0.05). In addition, the LPI was higher in the low- and moderate-

dose THH groups than in the high-dose THH group (*P* < 0.05), however, there was no significant difference in LPI between the low- and

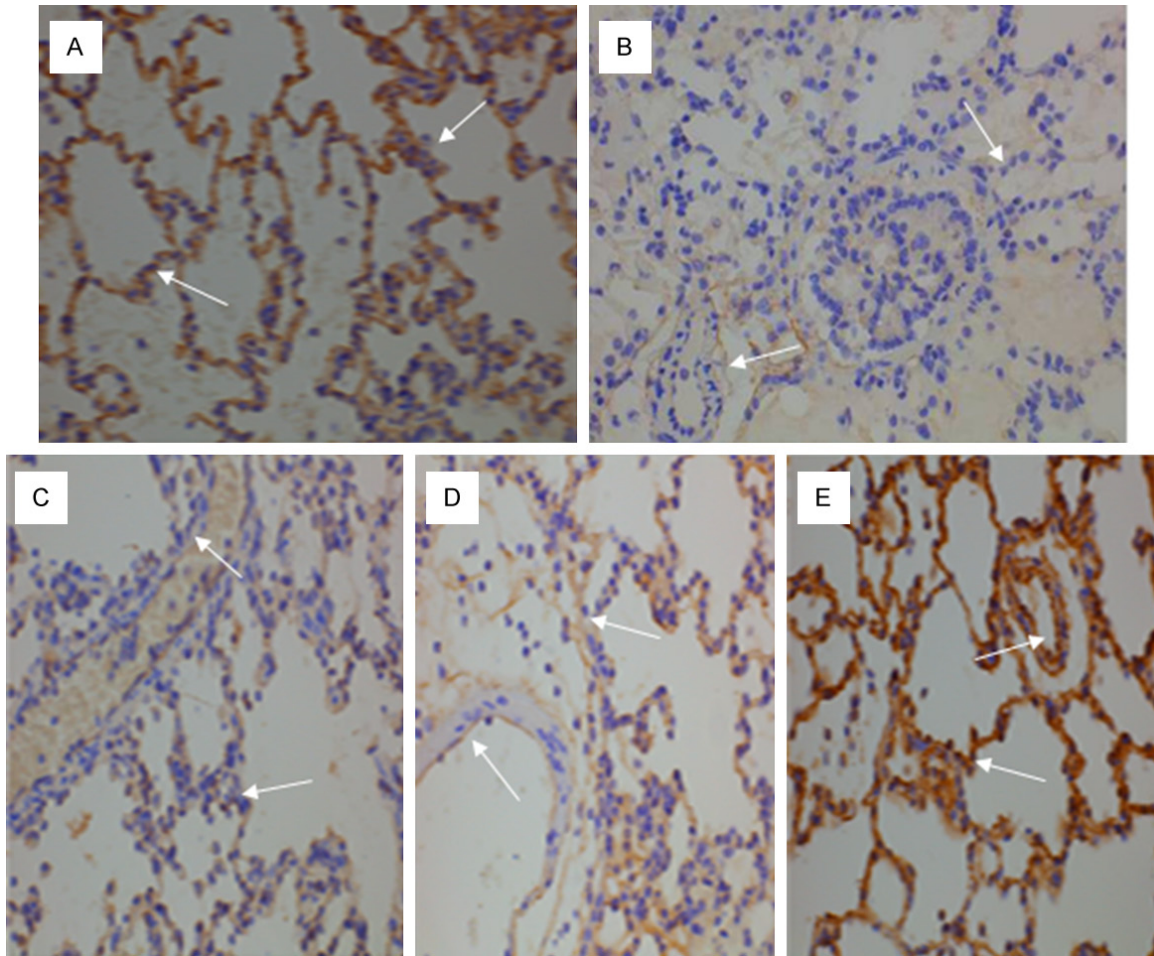


Figure 4. Immunohistochemical staining determines ZO-1 expression in rat lung tissues ($\times 400$). (A) Immunohistochemical staining shows moderate and highly positive ZO-1 expression (yellow brown) in alveolar endothelial cells, airway endothelial cells and vascular endothelial cells in the control group; (B) Immunohistochemical staining shows negative or weakly positive ZO-1 expression in the ALI group; (C-E) Immunohistochemical staining shows weak and moderately positive ZO-1 expression in the three THH groups, and higher ZO-1 expression was seen in the high-dose THH group (E) than in the low- (C) and moderate-dose THH groups (D).

moderate-dose THH groups ($P > 0.05$) (Table 2).

Effect of THH on claudin-5 and ZO-1 expression in lung tissues of rats with oleic acid-induced ALI

Claudin-5 is predominantly expressed in the pulmonary microvascular bed and alveolar capillary endothelial cells and is weakly expressed in pulmonary endothelial cells of rat lung tissues [24]. Immunohistochemistry revealed moderate and highly positive claudin-5 expression (yellow brown) in pulmonary vascular endothelial cells and weakly positive expression in alveolar endothelial cells in the control group, while negatively or weakly positive clau-

din-5 expression was determined in pulmonary vascular endothelial cells in the ALI group. Claudin-5 expression was found to increase with the rise in the THH dose in the pulmonary vascular endothelial cells, and the highest claudin-5 expression was determined in the high-dose THH group in relative to the low- and moderate-dose THH groups. In addition, weakly positive claudin-5 expression was detected in alveolar endothelial cells in the low-dose THH group, and the level of claudin-5 expression was comparable between the high-dose THH group and the control group. In addition, there was a significant difference in the area of lung tissues staining positively with claudin-5 among the five groups ($P < 0.05$) (Figure 3).

T. hypoglaucum attenuates acute lung injury

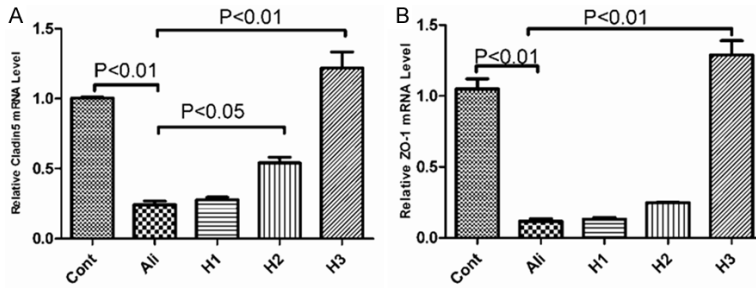


Figure 5. qRT-PCR assay detects claudin-5 (A) and ZO-1 mRNA expression (B) in rat lung tissues. Cont, the control group; Ali, the ALI group; H1, the low-dose THH group; H2, the moderate-dose THH group; H3, the high-dose THH group.

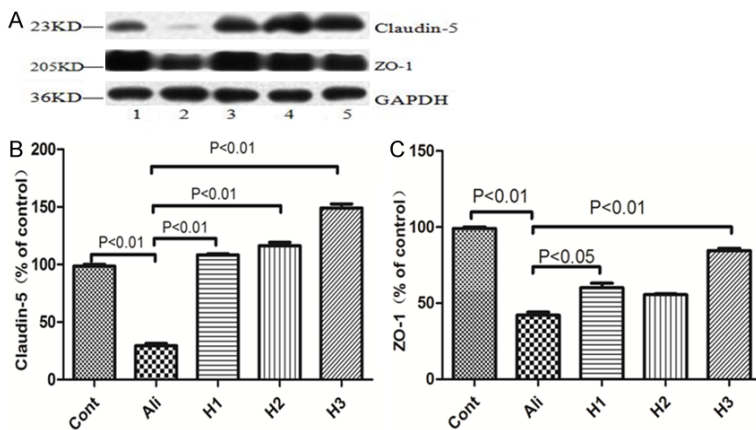


Figure 6. Western blotting analysis detects claudin-5 and ZO-1 expression in rat lung tissues. A. SDS-PAGE of claudin-5 and ZO-1 protein; B. Claudin-5 expression; C. ZO-1 expression. Cont, the control group; Ali, the ALI group; H1, the low-dose THH group; H2, the moderate-dose THH group; H3, the high-dose THH group.

As a tight junction protein, ZO-1 is highly expressed in alveolar epithelial cells and vascular epithelial cells, and poorly expressed in bronchial mucosal epithelial cells [25]. Immunohistochemical staining showed moderate and highly positive ZO-1 expression (yellow brown) in alveolar endothelial cells, airway endothelial cells and vascular endothelial cells in the control group, while negative or weakly positive ZO-1 expression was detected in the ALI group. Weak and moderately positive ZO-1 expression was seen in the three THH groups, and higher ZO-1 expression was seen in the high-dose THH group than in the low- and moderate-dose THH groups. In addition, there was a significant difference in the area of lung tissues staining positive for ZO-1 among the five groups ($P < 0.05$) (Figure 4).

After 4 h of animal modeling, qRT-PCR assay showed significantly lower claudin-5 and ZO-1

mRNA expression in the lung tissues in the ALI group than in the control group ($P < 0.01$), and higher claudin-5 and ZO-1 mRNA expression was observed in the high-dose THH group than in the ALI group ($P < 0.01$), while higher claudin-5 mRNA expression was detected in the moderate-dose THH group relative to the ALI group ($P < 0.05$). However, there were no significant differences in claudin-5 or ZO-1 mRNA expression between the other groups ($P > 0.05$) (Figure 5).

Western blotting analysis showed lower claudin-5 protein expression in the lung tissues in the ALI group than in the control group ($P < 0.01$), and higher claudin-5 protein expression in the three THH groups than in the ALI group ($P < 0.01$), while higher claudin-5 protein expression was detected in the high-dose THH group as compared to

the control group ($P < 0.05$). However, there were no significant differences in claudin-5 protein expression between other groups ($P > 0.05$) (Table 2, Figure 6A and 6B). ZO-1 protein expression was found to be lower in the lung tissues in the ALI group than in the control group ($P < 0.01$), and higher ZO-1 protein expression was seen in the low- ($P < 0.05$) and high-dose THH groups ($P < 0.01$) than in the ALI group, while the ZO-1 protein expression was higher in the high-dose THH group than in the low- ($P < 0.05$) and moderate-dose THH groups ($P < 0.01$). However, there were no significant differences in ZO-1 protein expression among other groups ($P > 0.05$) (Table 3, Figure 6A and 6C).

Discussion

The primary pathogenesis of ALI is persistent, uncontrolled inflammation caused by co-stimu-

Table 3. Expression of tight junction protein Claudin-5 and ZO-1 in rat lung tissues of various groups

Group	No. of animals	Claudin-5	ZO-1
Control	10	1.89 ± 0.66	2.82 ± 0.76
ALI	15	0.55 ± 0.50 [#]	1.25 ± 0.41 [#]
H1	15	2.03 ± 0.56 ^Δ	1.77 ± 0.69 ^{#,*}
H2	15	2.15 ± 0.61 ^Δ	1.56 ± 0.61 [#]
H3	15	2.89 ± 0.87 ^{*,Δ,▲,☆}	2.35 ± 0.51 ^{Δ,▲,☆}

[#]*P* < 0.01 vs. the control group; ^{*}*P* < 0.05 vs. the control group; ^Δ*P* < 0.01 vs. the ALI group; [▲]*P* < 0.05 vs. the H1 group; [☆]*P* < 0.05 vs. the H2 group; *indicates *P* < 0.05 vs. the control group.

lation with multiple inflammatory mediators and effector cells, which leads to secondary injury and diffuse parenchymal lung injury [26]. The common pathological alterations of excessive, uncontrolled pulmonary inflammatory response are acute diffuse injury of alveolar-capillary membrane and permeability pulmonary edema [27]. Pulmonary vascular endothelial and epithelial barrier functions may prevent pulmonary capillary leak and liquid entry into pulmonary alveolar cavity, and actively remove the exudation in the pulmonary alveolar cavity, therefore forming an important barrier to resist the formation of pulmonary edema [28]. The tight junction proteins in the pulmonary epithelial cells and vascular endothelial cells have been widely accepted critical to the stability of the pulmonary epithelial and vascular endothelial barrier [29]. The treatment approaches of ALI have been extensively investigated [5, 30, 31], and traditional Chinese medicines have been tested for their actions against ALI in animal models [32-34]. However, there is still lack of highly-effective and low-cost approaches available for the treatment of ALI. A search of novel therapies is therefore urgently needed and of great significance to improve the outcomes of ALI.

In this study, we established a rat model of ALI by administration of oleic acid at a dose of 0.04 ml/kg via the tail vein. All rats had cachexia, bradykinesia, dysphoria, dyspnea, and cyanosis 10 to 15 min post-injection, and the respiration rate increased to 100 to 120 beats per minute, with stridor found. In addition, pink liquid was found to overflow from the nasal cavity in rats with severe diseases. After 6 h of oleic acid administration, lung injury was seen at various degrees, which was manifested by enlargement of lung volume, poor lung elastic-

ty, patch bleeding below the envelop, and a great amount of pale red fluid exudates from the section. Optical microscopy revealed alveolar wall thickening, alveolar and pulmonary interstitial congestion and edema, inflammatory cell infiltration, red blood cell exudation, and alveolar collapse, while TEM showed typical alterations of pathological lung injury, including various degrees of bleeding in alveolar cavity, relatively irregular morphology of alveolar type

II epithelial cells, evacuation of lamellar body, inflammatory cell infiltration, organelle destruction, capillary endothelial injury, basement membrane thinning and disruption of intercellular tight junction structure. Following oleic acid administration, significantly higher lung W/D weight ratio, LIS and LPI were measured as compared to the controls (*P* < 0.01). These findings indicate that oleic acid treatment induces ALI in rats.

Tight junctions, a branching network of sealing strands on the top of epithelial and endothelial cells, with each strand acting independently from the others, join and seal intercellular space permeability and greatly determine the intercellular selective paracellular permeability. This structure is of great importance to maintain the normal morphology and function of the vascular endothelial barrier [35]. It has been reported that endothelial tight junction molecules are closely involved in pulmonary microvascular endothelial cell injury, vascular barrier dysfunction, and increased vascular permeability during ALI and ARDS [23, 36].

Claudin is an important tight junction transmembrane protein family containing 24 family members identified so far, and claudin-5, an important tight junction transmembrane protein, is highly expressed in alveolar capillary endothelial cells and lymphatic vessel and weakly expressed in alveolar epithelial cells [37, 38]. Aberrant claudin-5 expression may destroy pulmonary capillary endothelial cell barrier function [24]. A recent study detected significant silencing of claudin-5 in murine lung tissues with endotoxin-induced ALI, which affected pulmonary vascular endothelial barrier function, leading to extravasation of small molecules [39, 40]. It has been shown that claudin-5 deficiency results in an increase in

T. hypoglaucomum attenuates acute lung injury

selective permeability of the blood-brain barrier [41], and a decrease in the claudin-5 expression was detected in acute lung injury induced by intestinal ischemia-reperfusion [42], which demonstrates the important role of claudin-5 in the vascular endothelial barrier. In a mouse model of acrolein-induced ALI, a reduction in the claudin expression was found to correlate with the sensitivity to ALI [43]. In addition, the increase in the permeability of influenza virus-infected human pulmonary microvascular endothelial cells is reported to be strongly associated with claudin-5 degradation [44]. These findings indicate that claudin-5 expression is strongly associated with pulmonary permeability barrier function.

Scaffolding protein ZO-1, a cytoplasmic protein, is a tight junction protein that links claudin with intracellular cytoskeletal system and participates in the opening and closure of signal transduction and tight junctions, and down-regulation of ZO-1 expression results in a remarkable rise in the cell permeability [45]. Reduced ZO-1 expression was found to cause reduced transepithelial resistance, decreased epithelial barrier function, and elevated alveolar permeability [46]. Additionally, hypoxia has been shown to decrease ZO-1 and claudin-5 expression, cause the breakdown of vascular endothelial barrier function, and increase the vascular endothelial cell permeability [47]. In rats, disruption of the pulmonary epithelial barrier induced by hyperoxia was attributable to, at least in part, massive deterioration in the expression and localization of ZO-1 [25]. These findings demonstrate the critical physiological function of ZO-1 in maintaining the integrity of the vascular endothelial barrier [29].

In the present study, immunohistochemical staining showed a reduction in claudin-5 and ZO-1 expression in the lung tissues of rats with oleic acid-induced ALI, indicating that oleic acid administration causes aberrant claudin-5 expression in the capillary endothelial cells and abnormal ZO-1 expression in the cytoplasm in rat lung tissues. In addition, qRT-PCR assay and Western blotting analysis revealed significantly lower claudin-5 and ZO-1 expression in the ALI group than in the control rats at both transcriptional and translational levels ($P < 0.01$), suggesting that ALI causes vascular endothelial injury, destruction of the endotheli-

al structural integrity, a reduction in the claudin-5 and ZO-1 expression, which affects the stability of the tight junction, increases the vascular permeability and causes inflammatory exudation and tissue edema, thereby resulting in progressive hypoxia and inflammatory diffusion. Our findings demonstrate that pulmonary vascular endothelium and its transmembrane protein claudin-5 and scaffolding protein ZO-1 play critical roles in the endothelial barrier function.

THH, a traditional Chinese herbal medicine which has major ingredients including diterpenes, triterpenes, and alkaloids [48-50], has shown multiple pharmacological actions, including anti-inflammatory, immunosuppressive, anti-fertility, anti-viral, and anti-tumor activities [12-17]. However, to the best of our knowledge, the activity of THH against ALI remains unclear until now. This study was therefore designed with aims to investigate the *in vivo* activity of THH against oleic acid-induced ALI and explore the underlying mechanisms.

In this study, we found severe pathological injury in rat lung tissues and increases in higher lung W/D weight ratio, LIS, and LPI after injection with oleic acid via the tail vein. However, THH pretreatment resulted in a reduction in lung W/D weight ratio, LIS, and LPI, and optical microscopy showed alleviation of the pathological injury of the rat lung tissues following THH pretreatment. In addition, TEM revealed remarkable improvement in ultrastructural injury of the lung tissues, with almost normal structure of the alveolar wall, recovery of type II epithelial cells to normal, and apparent lamellar body in type II epithelial cells with normal organelle structure, normal capillary endothelial cell morphology with intact basement membrane, and obvious recovery of the integrity of the intercellular tight junction in the three THH groups. Our findings suggest that THH pretreatment remarkably restores the lung morphology and structure, decreases exudation from the alveolar cavity, alleviates inflammatory cell infiltration, and improves pulmonary edema and tissue injury in rats with ALI induced by oleic acid. In addition, greater alleviation of ALI was seen in the high-dose THH group than in the low- and moderate-dose THH groups, indicating that THH attenuates oleic acid-induced ALI in a dose-dependent manner. Immunohistochemi-

T. hypoglaucum attenuates acute lung injury

stry, qRT-PCR and Western blotting assays revealed higher claudin-5 and ZO-1 expression in the three THH groups than in the ALI group ($P < 0.01$). Our findings demonstrate that THH maintains the integrity of the vascular barrier in rats with ALI through up-regulating claudin-5 and ZO-1 expression, to ensure gas exchange and relieve hypoxemia, and THH treatment causes up-regulation of claudin-5 and ZO-1 expression to reduce capillary permeability, decrease inflammatory exudation and diffusion and prevent the aggravation of pulmonary edema.

In summary, the results of the present study demonstrate that THH attenuates pulmonary vascular endothelial cell injury caused by ALI through up-regulating claudin-5 and ZO-1 expression, and protects the pulmonary permeability barrier function in a dose-dependent manner. Our findings indicate that claudin-5 and ZO-1 may be potential targets for treatment of ALI, and provide new insights into the treatment of ALI.

Acknowledgements

The authors would like to thank Prof. Li Jing from the Department of Pathology, Prof. Yin Wang from the Department of Molecular Biology, and Prof. Jianqiang Yu from the School of Pharmacy, Ningxia Medical University for their kind help and assistance during the experiments. Thanks are also expressed to Prof. Zhongqin Guo from the Department of Biostatistics, Ningxia Medical University for the kind help during the data analysis. We sincerely thank Professors Xiangyuan Cao and Xiaohong Wang from the Department of Critical Care Medicine, the General Hospital of Ningxia Medical University for their valuable comments on our manuscript. This study was supported by the grants from the National Natural Science Foundation of China (grant no. 81260583) and the Natural Science Foundation of Ningxia Hui Autonomous Region (grant no. NZ10139).

Disclosure of conflict of interest

None.

Address correspondence to: Xigang Ma, Department of Critical Care Medicine, General Hospital of Ningxia Medical University, 804 Shenglii South Street, Xingqing District, Yinchuan City 750004,

Ningxia Hui Autonomous Region, China. Tel: +86-951-6744356; Fax: +86-951-4082981; E-mail: nyfyicu@163.com

References

- [1] Tsushima K, King LS, Aggarwal NR, De Gorordo A, D'Alessio FR, Kubo K. Acute lung injury review. *Intern Med* 2009; 48: 621-630.
- [2] Rubenfeld GD, Caldwell E, Peabody E, Weaver J, Martin DP, Neff M, Stern EJ, Hudson LD. Incidence and outcomes of acute lung injury. *N Engl J Med* 2005; 353: 1685-1693.
- [3] Johnson ER, Matthay MA. Acute lung injury: epidemiology, pathogenesis, and treatment. *J Aerosol Med Pulm Drug Deliv* 2010; 23: 243-252.
- [4] Ware LB, Matthay MA. The acute respiratory distress syndrome. *N Engl J Med* 2000; 342: 1334-1349.
- [5] Wheeler AP, Bernard GR. Acute lung injury and the acute respiratory distress syndrome: a clinical review. *Lancet* 2007; 369: 1553-1564.
- [6] Amato MB, Barbas CS, Medeiros DM, Magaldi RB, Schettino GP, Lorenzi-Filho G, Kairalla RA, Deheinzelin D, Munoz C, Oliveira R, Takagaki TY, Carvalho CR. Effect of a protective-ventilation strategy on mortality in the acute respiratory distress syndrome. *N Engl J Med* 1998; 338: 347-354.
- [7] Chiche L, Forel JM, Papazian L. Low-tidal-volume ventilation. *New Engl J Med* 2008; 357: 2519-2520.
- [8] Malhotra A. Low-tidal-volume ventilation in the acute respiratory distress syndrome. *New Engl J Med* 2007; 357: 1113-1120.
- [9] Pelosi P, Rocco PRM, Vincent JL. Glucocorticoid treatment in acute respiratory distress syndrome: friend or foe? *Intensive Care Med* 2008; 2008: 214-223.
- [10] Gibbs RH. Glucocorticoid therapy in acute respiratory distress syndrome. *Br J Hosp Med (Lond)* 2009; 70: 665.
- [11] Marik PE, Meduri GU, Rocco PR, Annane D. Glucocorticoid treatment in acute lung injury and acute respiratory distress syndrome. *Crit Care Clin* 2011; 27: 589-607.
- [12] Liang ZQ, Cao N, Song ZK, Wang X. *In vitro* porcine brain tubulin assembly inhibition by water extract from a Chinese medicinal herb, *Tripterygium hypoglaucum* Hutch. *World J Gastroenterol* 2006; 12: 1133-1135.
- [13] Jiang X, Huang XC, Ao L, Liu WB, Han F, Cao J, Zhang DY, Huang CS, Liu JY. Total alkaloids of *Tripterygium hypoglaucum* (levl.) Hutch inhibits tumor growth both *in vitro* and *in vivo*. *J Ethnopharmacol* 2014; 151: 292-298.
- [14] Duan H, Takaishi Y, Imakura Y, Jia Y, Li D, Cosentino LM, Lee KH. Sesquiterpene alka-

T. hypoglaucum attenuates acute lung injury

- loids from *Tripterygium hypoglaucum* and *Tripterygium wilfordii*: a new class of potent anti-HIV agents. *J Nat Prod* 2000; 63: 357-361.
- [15] Ren Z, Zhang CH, Wang LJ, Cui YX, Qi RB, Yang CR, Zhang YJ, Wei XY, Lu DX, Wang YF. *In vitro* anti-viral activity of the total alkaloids from *Tripterygium hypoglaucum* against herpes simplex virus type 1. *Virologica Sinica* 2010; 25: 107-114.
- [16] Zhang YW, Fan YS, Wang XD, Gao WY, Duan HQ. Diterpenoids possessed immunosuppressive activity from *Tripterygium hypoglaucum*. *Chin Tradit Herb Drugs* 2007; 38: 493-496.
- [17] Wang D, Guo YW, Shi DZ. Antifertility effects of crude ethanol extracts of *Tripterygium hypoglaucum* (Levl.) Hutch in male *Mongolian gerbils*. *J Appl Animal Res* 2011; 39: 44-48.
- [18] Liu Y, Guan JH. Clinical observation of radix tripterygium hypoglaucum tablet in treating refractory nephrotic syndrome. *Chin J Integr Tradit West Nephrol* 2003; 4: 47.
- [19] Chen YX, Hu JF, Qiao Y, Qiao HM. Clinical efficacy of *Tripterygium hypoglaucum* (Level) Hutch in rheumatoid arthritis. *Military Med J South China* 2009; 23: 4-6.
- [20] Lin LM, Qi XM. Comparative observation on the effects of Radix tripterygium hypoglaucum tablet and *Tripterygium glycosides* tablet in treating erosive oral lichen planus. *Chin J Integr Med* 2005; 11: 149-150.
- [21] Zhang Y, Fang YF, Wang Y. Research on the advances in the pharmacological actions and clinical applications of *Tripterygium glycosides*. *People Mil Surg* 2008; 51: 463-464.
- [22] Bastarache JA, Blackwell TS. Development of animal models for the acute respiratory distress syndrome. *Dis Model Mech* 2009; 2: 218-223.
- [23] Sun C, Beard RS Jr, McLean DL, Rigor RR, Konia T, Wu MH, Yuan SY. ADAM15 deficiency attenuates pulmonary hyperpermeability and acute lung injury in lipopolysaccharide-treated mice. *Am J Physiol Lung Cell Mol Physiol* 2013; 304: L135-L142.
- [24] Paschoud S, Bongiovanni M, Pache JC, Citi S. Claudin-1 and claudin-5 expression patterns differentiate lung squamous cell carcinomas from adenocarcinomas. *Mod Pathol* 2007; 20: 947-954.
- [25] You K, Xu X, Fu J, Xu S, Yue X, Yu Z, Xue X. Hyperoxia disrupts pulmonary epithelial barrier in newborn rats via the deterioration of occludin and ZO-1. *Respir Res* 2012; 13: 36.
- [26] Ware LB. Pathophysiology of acute lung injury and the acute respiratory distress syndrome. *Semin Respir Crit Care Med* 2006; 27: 337-349.
- [27] Chen F, Fan XH, Wu YP, Zhu JL, Wang F, Bo LL, Li JB, Bao R, Deng XM. Resolvin D1 improves survival in experimental sepsis through reducing bacterial load and preventing excessive activation of inflammatory response. *Eur J Clin Microbiol Infect Dis* 2014; 33: 457-464.
- [28] Lucas R, Verin AD, Black SM, Catravas JD. Regulators of endothelial and epithelial barrier integrity and function in acute lung injury. *Biochem Pharmacol* 2009; 77: 1763-1772.
- [29] González-Mariscal L, Betanzos A, Nava P, Jaramillo BE. Tight junction proteins. *Prog Biophys Mol Biol* 2003; 81: 1-44.
- [30] Marinelli WA, Ingbar DH. Diagnosis and management of acute lung injury. *Clin Chest Med* 1994; 15: 517-546.
- [31] Seeley EJ. Updates in the management of acute lung injury: a focus on the overlap between AKI and ARDS. *Adv Chronic Kidney Dis* 2013; 20: 14-20.
- [32] Gao Z, Xu J, Sun D, Zhang R, Liang R, Wang L, Fan R. Traditional Chinese medicine, Qing Ying Tang, ameliorates the severity of acute lung injury induced by severe acute pancreatitis in rats via the upregulation of aquaporin-1. *Exp Ther Med* 2014; 8: 1819-1824.
- [33] Li CW, Chen ZW, Wu XL, Ning ZX, Su ZQ, Li YC, Su ZR, Lai XP. A standardized traditional Chinese medicine preparation named Yejuhua capsule ameliorates lipopolysaccharide-induced acute lung injury in mice via downregulating toll-like receptor 4/nuclear factor- κ B. *Evid Based Complement Alternat Med* 2015; 2015: 264612.
- [34] Yeh CC, Lin CC, Wang SD, Chen YS, Su BH, Kao ST. Protective and anti-inflammatory effect of a traditional Chinese medicine, Xia-Bai-San, by modulating lung local cytokine in a murine model of acute lung injury. *Int Immunopharmacol* 2006; 6: 1506-1514.
- [35] Tsukita S, Furuse M, Itoh M. Multifunctional strands in tight junctions. *Nat Rev Mol Cell Biol* 2001; 2: 285-293.
- [36] Tomashefski JF Jr. Pulmonary pathology of acute respiratory distress syndrome. *Clin Chest Med* 2000; 21: 435-466.
- [37] Koval M. Claudin heterogeneity and control of lung tight junctions. *Annu Rev Physiol* 2013; 75: 551-567.
- [38] Mitchell LA, Ward C, Kwon M, Mitchell PO, Quintero DA, Nusrat A, Parkos CA, Koval M. Junctional adhesion molecule A promotes epithelial tight junction assembly to augment lung barrier function. *Am J Pathol* 2015; 185: 372-386.
- [39] Chen W, Sharma R, Rizzo AN, Siegler JH, Garcia JG, Jacobson JR. Role of claudin-5 in the attenuation of murine acute lung injury by simvastatin. *Am J Respir Cell Mol Biol* 2014; 50: 328-336.
- [40] Jang AS, Concel VJ, Bein K, Brant KA, Liu S, Pope-Varsalona H, Dopico RA Jr, Di YP, Knoell DL, Barchowsky A, Leikauf GD. Endothelial dys-

T. hypoglaucum attenuates acute lung injury

- function and claudin 5 regulation during acrolein-induced lung injury. *Am J Respir Cell Mol Biol* 2011; 44: 483-490.
- [41] Nitta T, Hata M, Gotoh S, Seo Y, Sasaki H, Hashimoto N, Furuse M, Tsukita S. Size-selective loosening of the blood-brain barrier in claudin-5-deficient mice. *J Cell Biol* 2003; 161: 653-660.
- [42] Jing H, Yao J, Liu X, Fan H, Zhang F, Li Z, Tian X, Zhou Y. Fish-oil emulsion (omega-3 polyunsaturated fatty acids) attenuates acute lung injury induced by intestinal ischemia-reperfusion through adenosine 5'-monophosphate-activated protein kinase-sirtuin1 pathway. *J Surg Res* 2014; 187: 252-261.
- [43] Jang AS, Concel VJ, Bein K, Brant KA, Liu S, Pope-Varsalona H, Dopico RA Jr, Di YP, Knoell DL, Barchowsky A, Leikauf GD. Endothelial dysfunction and claudin 5 regulation during acrolein-induced lung injury. *Am J Respir Cell Mol Biol* 2011; 44: 483-490.
- [44] Armstrong SM, Wang C, Tigdi J, Si X, Dumpit C, Charles S, Gamage A, Moraes TJ, Lee WL. Influenza infects lung microvascular endothelium leading to microvascular leak: role of apoptosis and claudin-5. *PLoS One* 2012; 7: e47323.
- [45] Huang YJ, Feng JC. Study of zonula occluden-1. *Neural Regen Res* 2006; 1: 553-556.
- [46] Mitchell LA, Ward C, Kwon M, Mitchell PO, Quintero DA, Nusrat A, Parkos CA, Koval M. Junctional adhesion molecule A promotes epithelial tight junction assembly to augment lung barrier function. *Am J Pathol* 2015; 185: 372-386.
- [47] Ma X, Zhang H, Pan Q, Zhao Y, Chen J, Zhao B, Chen Y. Hypoxia/Aglycemia-induced endothelial barrier dysfunction and tight junction protein downregulation can be ameliorated by citico-line. *PLoS One* 2013; 8: e82604.
- [48] Zhang L, Zhang ZX, Sheng LS, An DK, Lu Y, Zheng QT, Wang SC. Study on the chemical constituents of *Tripterygium hypoglaucum* (Lévl.) Hutch. *Acta Pharm Sin* 1993; 28: 32-34.
- [49] Liu Z, Zhao R, Zou Z. Chemical constituents from root bark of *Tripterygium hypoglaucum*. *China J Chin Materia Med* 2011; 36: 2503-2506.
- [50] Jiang X, Huang XC, Ao L, Liu WB, Han F, Cao J, Zhang DY, Huang CS, Liu JY. Total alkaloids of *Tripterygium hypoglaucum* (levl.) Hutch inhibits tumor growth both *in vitro* and *in vivo*. *J Ethnopharmacol* 2014; 151: 292-298.